Vortex lattice transitions in borocarbides

V. G. Kogan, M. Bullock, and B. Harmon
Ames Laboratory DOE and Department of Physics, Iowa State University, Ames, Iowa 50011

P. Miranović and Lj. Dobrosavljević-Grujić
Institute of Physics, P.O. Box 57, 11001 Belgrade, Yugoslavia

P. L. Gammel and D. J. Bishop
Bell Laboratories, Lucent Technologies, Murray Hill, New Jersey 07974

(Received 6 January 1997)

Nonlocal corrections to the London model are used to describe vortex lattices in $LuNi_2B_2C$. Within this scheme in fields along the c axis, vortices should form a square lattice (rotated 45° relative to the crystal axes a and b) at large fields, should transform to a triangular one at a field H_2, and to another triangular lattice at a still lower field H_1. We argue that the transition at H_2 is of second order, whereas at H_1 it is of first order. In tilted fields, H_2 is predicted to move to higher fields. Neutron-scattering data for $ErNi_2B_2C$ are discussed. [S0163-1829(97)52414-3]

The growth of large high-quality crystals of borocarbides (RE=Er,Y,Lu)Ni_2B_2C has stimulated studies of vortex lattices (VL) in these superconductors by small-angle neutron scattering (SANS), scanning tunneling microscopy (STM), and decoration experiments. For all of these high-κ materials, in magnetic fields along [001], SANS show a square VL with one side parallel to [110] at fields higher than 2 kG (the square rotated 45° relative to the crystal);[1–3] the same VL is seen with STM on $LuNi_2B_2C$.[4] As the field is reduced below a temperature and material-dependent value H_2 (in the 0.3–1 kG range) this VL transforms into a near hexagonal lattice made of rhombic cells with diagonals along [100] and [010]. This transition field increases with increasing temperature. The transformation proceeds via a rhombohedral distortion of the square which preserves the orientations of the diagonals along [100] and [010] and, of course, the unit cell area due to flux quantization.[2]

In this paper we study VL's in $LuNi_2B_2C$ in some detail as a representative of nonmagnetic borocarbides. We show that the London model amended with nonlocal corrections accounts for most of the observed features, among which the conspicuous square-to-triangle transition is currently under intensive experimental scrutiny.

The idea that the nonlocality of the relation between the current density $\mathbf{j}$ and the vector potential $\mathbf{A}$ in superconductors[5,6] plays a role in forming VL's is not new.[7] The nonlocality is caused by the finite size, ξ_0, of Cooper pairs. Instead of local relations between $\mathbf{j}$ and $\mathbf{A}$ of the Ginzburg-Landau (GL) or London (L) approaches, the microscopic theory provides an integral equation with a kernel $\hat{Q}$ extending to distances $\sim\xi_0$; in Fourier space this relation is of the form $\mathbf{j}(\mathbf{k})=\hat{Q}(\mathbf{k})\mathbf{A}(\mathbf{k})$.[6] In the GL domain where $\xi(T)\gg\xi_0$, or far from the vortex cores, the nonlocal corrections vanish.

It is hard to utilize the microscopic theory as it is formulated for the VL problem. It is also not easy to justify the nonlocal contributions to the GL theory (higher-order gradients) to describe the VL data taken at temperatures far from T_c and in fields well under the upper critical field H_{c2}. Usually, for materials with a large GL parameter κ, the L approach is quite adequate for T's and H's relevant for VL's. In particular, this simple approach reproduces well the main features of the coupling between VL's and the underlying anisotropic crystal structure.[8,9] Still, there are many examples when the L model fails; cubic superconductors are among them. Since both L and GL theories incorporate crystal anisotropy via the second-rank mass tensor m_{ik}, within these approaches, the cubic crystals should behave as isotropic, i.e., VL's should be hexagonal for any field orientation. This, however, is not the case as has been shown in SANS experiments on cubic superconductors.[7,10,11] Thus, the idea of developing the nonlocal corrections to the L theory for description of VL's at $T\ll T_c$ and $H<H_{c2}$ is more promising than the similar one within GL.

The corrections have recently been derived to address the problem of low-T magnetization in high-T_c materials.[12] The idea was to take the general form of $\hat{Q}(\mathbf{k})$ (which is $\propto\lambda^{-2}$ for $k\to 0$ with λ being the penetration depth) and expand it in the small parameter $k^2\xi_0^2$. The corrections were applied successfully[13] to describe the data on VL's in cubic V_3Si.[11]

Having in mind application to the tetragonal $LuNi_2B_2C$, we start with the general form of these corrections:[12]

$$\frac{4\pi}{c}j_i=-\frac{1}{\lambda^2}(m_{ij}^{-1}-\lambda^2 n_{ijlm}k_l k_m)a_j\,. \tag{1}$$

Here, $\mathbf{a}=\mathbf{A}+\phi_0\nabla\theta/2\pi$, θ is the order-parameter phase, and ϕ_0 is the flux quantum. The inverse ''mass tensor'' $m_{ij}^{-1}=\langle v_i v_j\rangle/(\det\langle v_i v_j\rangle)^{1/3}$ is defined so as $\det m_{ij}=1$; $\mathbf{v}$ is the Fermi velocity, and $\langle\cdots\rangle$ stands for the average over the Fermi surface. Further, $\lambda=(\lambda_a\lambda_b\lambda_c)^{1/3}$ is the average penetration depth and $\lambda_i=\lambda\sqrt{m_i}$ with $i=a,b,c$. Summation is

implied over repeated subscripts. Denoting $D=(\det\langle v_i v_j\rangle)^{1/3}$ (in the isotropic or cubic case $D=\langle v^2\rangle/3$) we have[12]

$$n_{ijlm}=\frac{\hbar^2\langle v_i v_j v_l v_m\rangle}{4D\Delta_0^2\lambda^2}\gamma, \quad \gamma=\frac{\Delta_0^2\Sigma\beta_0^{-2}(\beta')^{-3}}{\Sigma\beta_0^{-2}(\beta')^{-1}}. \tag{2}$$

Here, $\beta_0^2=\Delta_0^2+\hbar^2\omega^2$, $\Delta_0(T)$ is the energy gap, $\hbar\omega=\pi T(2n+1)$ with an integer n, and the sums in γ are extended to $\omega>0$. Further, $\beta'=\beta_0+\hbar/2\tau$ with τ being the scattering time due to nonmagnetic impurities. Note that tensor $\hat{n}$ is symmetric in all indices.

The quantity $\gamma(T,\tau)$ was evaluated in Ref. 12; in the clean limit $\gamma=2/3$ at $T=0$ and drops to ≈ 0.30 at T_c. Scattering suppresses γ; in the dirty limit $\gamma\to(\tau\Delta_0/\hbar)^2\to 0$, i.e., nonlocal effects vanish. Thus, $n\sim\xi_0^2/\lambda^2\sim\kappa^{-2}$ in the clean case and is of the order $(v\tau/\lambda)^2$ for dirty materials.

With $\hat{n}=0$, Eq. (1) is the standard anisotropic L equation.[14] Being dependent on the shape of the Fermi surface, the fourth-rank tensor $\hat{n}$ couples supercurrents with the crystal even in cubic materials. For a tetragonal symmetry in the crystal frame (a,b,c), m_{ij}^{-1} is diagonal with two different eigenvalues $m_{aa}^{-1}=m_{bb}^{-1}=1/m_a$ and $m_{cc}^{-1}=1/m_c$, whereas $\hat{n}$ has four independent components $n_1=n_{aaaa}$, $n_2=n_{aabb}$, $n_3=n_{cccc}$, and $n_4=n_{aacc}$. To evaluate $\hat{m}$ and $\hat{n}$ one needs Fermi-surface averages of products of Fermi velocities; therefore, one turns to the band structure of $LuNi_2B_2C$.

The Fermi-surface averages for the relevant products of velocities were evaluated using an accurate tight-binding fit[15] to the first-principles linearized augmented plane-wave calculations.[16] To obtain the velocities, the Brillouin zone was divided into tetrahedrons and the energy eigenvalues were determined at each corner. Linear interpolation was used to obtain the Fermi surface in the 919 tetrahedrons which had bands crossing the Fermi level (out of the total number of 1536). For those bands, the velocity at the k point centered on each piece of Fermi surface was determined numerically, and added to obtain the appropriate averages:

$$\langle v^2\rangle=5.12\times10^{14}\ \ (\mathrm{cm/sec})^2,$$

$$\langle v_a^4\rangle=1.44\times10^{29}\ \ (\mathrm{cm/sec})^4,$$

$$\langle v_a^2 v_b^2\rangle=1.85\times10^{28}\ \ (\mathrm{cm/sec})^4,$$

$$\langle v_c^4\rangle=5.85\times10^{28}\ \ (\mathrm{cm/sec})^4,$$

$$\langle v_a^2 v_c^2\rangle=1.97\times10^{28}\ \ (\mathrm{cm/sec})^4. \tag{3}$$

Besides, $\langle v_a^2\rangle=1.87\times10^{14}$ $(\mathrm{cm/sec})^2$, which yields $m_{aa}\equiv m_a=0.904$ and $m_{cc}\equiv m_c=1.22$ that agrees with a weak anisotropy of H_{c2} seen in this material.[17]

Now one can evaluate $\hat{n}$ provided Δ_0,λ, and τ are given. Since none of these are known with sufficient accuracy, we combine them in one parameter $C(T,\tau)$:

$$n_{ijlm}=C\frac{\langle v_i v_j v_l v_m\rangle}{\langle v^2\rangle^2}, \quad C=\frac{\hbar^2\langle v^2\rangle^2\gamma}{4D\Delta_0^2\lambda^2}. \tag{4}$$

With the averages (3) we have

$$n_1=0.549C, \quad n_2=0.0705C,$$

$$n_3=0.223C, \quad n_4=0.0751C. \tag{5}$$

For the material in the clean limit and $\lambda\approx 710$ Å,[18] we estimate $C\approx 0.363$. To fit the experimentally observed ''square-to-triangle'' transition at ≈ 500 G, we need $C\approx 0.221$, the value to be employed in all data analyses on the Lu system.

We now apply Eq. (1) to a vortex along some direction z. To find the field component h_z (the only one needed for evaluating intervortex interaction $\phi_0 h_z/4\pi$), one has to invert Eq. (1) to isolate **a**, and use the flux quantization condition, $\mathrm{curl}\,\mathbf{a}=\mathbf{h}-\phi_0\hat{z}\,\delta(\mathbf{r})$. To this end, we write Eq. (1) in the form $(4\pi\lambda^2/c)j_i=-q_{ij}a_j$ with $q_{ij}=m_{ij}^{-1}-\lambda^2 N_{ij}$ and $N_{ij}=n_{ijlm}k_l k_m$. Since the correction $\lambda^2 N_{ij}$ is small, one finds $q_{ij}^{-1}=m_{ij}+\lambda^2 m_{is}m_{jt}N_{st}$. After straightforward algebra we have

$$h_i+\lambda^2 e_{lst}e_{kni}q_{lk}^{-1}k_n k_s h_t=\phi_0\hat{z}_i, \tag{6}$$

where e_{ikl} is the unit antisymmetric tensor. This reduces to the anisotropic London equation when the nonlocal corrections are absent and $q_{ij}^{-1}=m_{ij}$.[14] The system of three equations (6) can be solved for h_i's for a general vortex orientation; instead we focus below on two simple situations, the applied field along c and a.

The free-energy density of a VL directed along z is

$$F=B^2\sum_{\mathbf{g}} h_z(\mathbf{g})/8\pi\phi_0, \tag{7}$$

where B is the magnetic induction and h_z is taken at wave vectors $\mathbf{k}=\mathbf{g}$ forming a proper reciprocal lattice. The equilibrium VL at a given **H** corresponds to the minimum of $G=F-\mathbf{BH}/4\pi$. Dealing with different sample shapes in a given *applied* field, one should define a proper potential which is a minimum in equilibrium. We focus here on the case of the applied field perpendicular to a platelet sample and parallel to one of the principal crystal directions; equilibrium VL's are then given by the absolute minimum of F at a given B.

We start with **H** along [001]; the vortex field has only one component h_z. We choose the coordinates (x,y,z) coinciding with the crystal frame (a,b,c). Then all tensors are easily evaluated, e.g., $q_{\mu\nu}^{-1}=m_a(\delta_{\mu\nu}+\lambda_{ab}^2 N_{\mu\nu})$ where the greek indices take only x,y values. We obtain after simple algebra

$$h_z[1+\lambda_{ab}^2k^2+\lambda_{ab}^4(n_2k^4+dk_x^2k_y^2)]=\phi_0,$$

$$d=2n_1-6n_2. \tag{8}$$

One can verify that in the isotropic case $d=0$; thus $d\neq 0$ is responsible for the anisotropy. We note that although the fourth-order terms in Eq. (8) make the sum (7) formally convergent, the L approach (with or without nonlocal corrections) fails in the vortex core, and one has to introduce a cutoff at $g\sim 1/\xi$. Minimization of the energy for this case is done by complementing $h_z(\mathbf{g})$ with a factor $\exp(-g^2\xi^2)$.[13]

In comparing energies for various VL's, we note that for the case in question, the field and the crystal have (100) and (110) symmetry planes. We will look for VL's having one of these symmetry elements. Thus, the general parallelogram of

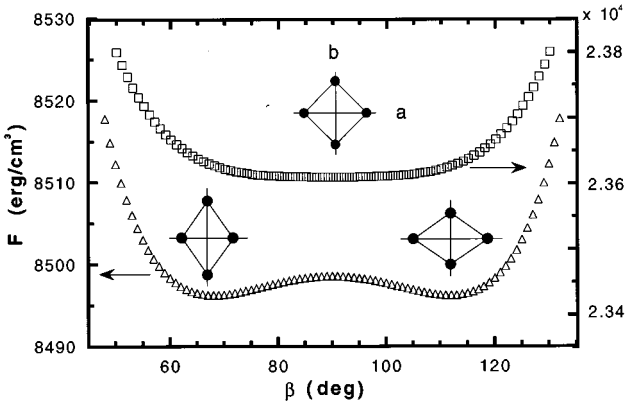

FIG. 1. The free-energy F vs the apex angle β of a rhombic unit cell in fields 200 G (the lower curve) and 500 G (the upper curve) parallel to $\hat{c}$. For $H<H_2\approx 480$ G, two minima at $\beta'>60°$ and $\beta''<120°$ approach each other with increasing field and merge at $H=H_2$ to $\beta=90°$. The square VL remains stable for $H>H_2$.

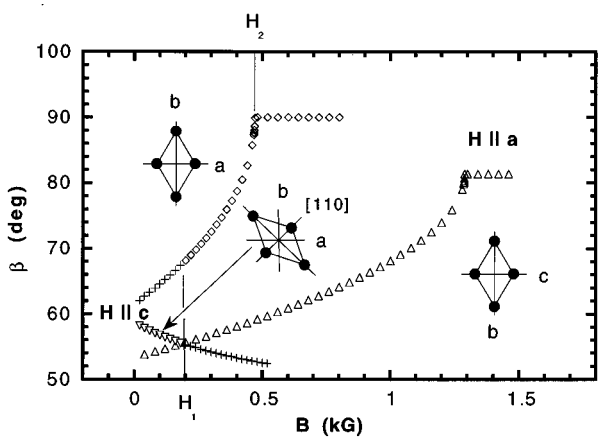

FIG. 2. The apex angle β of rhombic unit cells vs applied fields. Two curves on the left are for $\mathbf{H}\|\hat{c}$. The upper curve is for the rhombus diagonals along a,b [examples of $F(\beta)$ for this case are given in Fig. 1]. The lower-left curve is for rhombic VL's with a diagonal along [110]; these VL's are unstable for $H>H_1$ where they are shown by crosses. The curve starting at the right is for $\mathbf{H}\|\hat{a}$; the structure shown is stable.

the VL unit cell is reduced to a rhombus with a diagonal along [100] or [110]. We will minimize F for each of these possibilities separately and choose the energetically favorable. We will see that whichever case wins depends on H. The VL vectors for the first possibility are $\mu\mathbf{b}_1+\nu\mathbf{b}_2$ with integers μ,ν and $\mathbf{b}_1=b(\hat{\mathbf{x}}\sin\beta_1+\hat{\mathbf{y}}\cos\beta_1)$, $\mathbf{b}_2=b(-\hat{\mathbf{x}}\sin\beta_1+\hat{\mathbf{y}}\cos\beta_1)$; b is the side of the isosceles triangle and $2\beta_1=\beta$ is the apex angle: $b=\sqrt{\phi_0/B\sin\beta}$. The reciprocal lattice is $g_{1x}=\pi(\mu-\nu)/b\sin\beta_1$, $g_{1y}=\pi(\mu+\nu)/b\cos\beta_1$. For the second possibility, [110] is the rhombus diagonal: $g_{2x}=2\pi(\nu\cos\beta_2-\mu\sin\beta_2)/b\sin\beta$, $g_{2y}=2\pi(\mu\cos\beta_2-\nu\sin\beta_2)/b\cos\beta$, with $\beta_2=\beta/2-\pi/4$.

Examples of $F(\beta)$ are shown in Fig. 1. The angles β obtained by minimizing F at different fields are shown in Fig. 2. At small fields, the minimum energy corresponds to the rhombus with a diagonal along [110]; this structure becomes unstable at $H_1\approx 180$ G. For $H>H_1$, the equilibrium rhombus has a diagonal along [100], shown at the left of Fig. 2. The transition at H_1 cannot be realized by a small deformation; i.e., it is of the first order. The situation near $H_2\approx 480$ G is different: as $H\to H_2$ from below, the angle $\beta\to 90°$ while the orientation of the rhombus does not change. The transition at H_2 to a square VL is therefore of the second order.

It should be noted that due to the fourfold rotational symmetry ($\hat{c}$) for this field orientation, each structure mentioned above can be rotated 90° without changing the energy. The existence of structures with equal or close energies may result in domains of different VL's or cause disorder in actual vortex arrangements.

The treatment is more involved for an arbitrary field orientation, since $\hat{m}$ and $\hat{n}$ have to be transformed from the crystal frame where $\hat{m}$ is diagonal and $\hat{n}$ is given by Eq. (5), to the frame (x,y,z) with z along the vortex axes. To avoid this formal complexity, we demonstrate the effect of tilted fields for the simple situation of $\mathbf{H}\|\hat{a}$. We choose the axes so that $x=c$, $y=b$, and $z=a$; then the needed components of $\hat{n}$ are $n_{xxxx}=n_{cccc}=n_3$, $n_{yyyy}=n_{bbbb}=n_1$, and $n_{xxyy}=n_{ccaa}=n_4$. For $\mathbf{H}\|\hat{a}$, the symmetry planes of the crystal and field are (010) or (001); the only rhombus compatible with these elements is one with diagonals at [001] and [010]; see Fig. 2. Proceeding as in the previous case we obtain

$$h_z[1+\lambda^2K^2+\lambda^4(n_4K^4+dk_x^2k_y^2)]=\phi_0, \tag{9}$$

$$K^2=m_ak_x^2+m_ck_y^2, \quad d=n_3m_c^2+n_1m_a^2-6n_4m_am_c.$$

Results of minimization of the energy (7) with this h_z are shown in Fig. 2. A few points are to be noticed: (a) Due to the anisotropy in the xy (or bc) plane, the high-field structure is not a 45° rotated square but a rhombus with the apex angle $\beta\approx 81.3°$ of the same orientation. The low-field VL is made of an isosceles triangles even in the limit $B\to 0$. (b) Unlike the case $\mathbf{H}\|\hat{c}$, we have here only two competing rhombic VL's in low fields. Still, we expect the low-field VL in this case to be better ordered than for $\mathbf{H}\|\hat{c}$. (c) The transition between the fixed high-field structure and the B dependent low-field VL occurs at $H_2=1.25$ kG as compared to about 0.5 kG for $\mathbf{H}\|\hat{c}$. The last feature might be interpreted qualitatively as follows: the high-field locked structure is caused by nonlocal effects with a range of the order ξ_0. The smaller this range, the weaker the nonlocal effect, and the locking happens at shorter intervortex distances, i.e., at higher fields. For anisotropic materials, the role of ξ_{ab}^2 for $\mathbf{H}\|\hat{c}$ goes to $\xi_b\xi_c$ when $\mathbf{H}\|\hat{a}$, so that the effective range shrinks ($\xi_c<\xi_{ab}$) while the transition to a locked state moves to higher fields. Since the nonlocality range slowly decreases with raising T, one expects the transition field H_2 to increase with temperature. The increasing transition field qualitatively agrees with experiments on the Er and Lu systems, although the data are not yet accurate enough for a detailed comparison.

The predictions we make on VL transitions for the Lu compound are not yet properly verified since so far we do

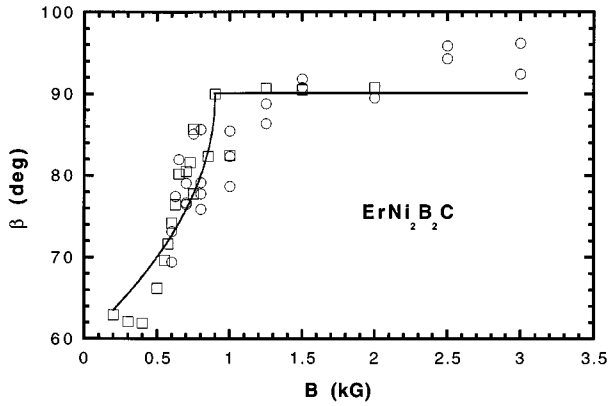

FIG. 3. The apex angle β of rhombic unit cells vs applied fields parallel to $\hat{c}$ from the SANS data on $ErNi_2B_2C$ at $T=3.5$ K. The circles are taken from $\theta-2\theta$ scans. The squares are taken from the location of the Bragg reflections on an area detector at the peak of the rocking curve. The scatter in the data accurately represents the error bars. The solid line is calculated assuming $H_2\approx 900$ G.

not have the data needed. The model, however, does not contradict the data on the Er compound as indicated in Fig. 3. Although we do not possess at the moment the Fermi averages (3) which make the model quantitative, the data suggest the transition field H_2 as ≈ 900 G. This allows us to reconstruct the low-field part of the curve $\beta(B)$ in a reasonable agreement with data.

Thus, we have shown that the London model corrected for nonlocal effects accounts well for the square VL's seen in high fields parallel to the $\hat{c}$ axis of borocarbides. The model explains the observed transition to triangular structures with the field reduction. More data are needed to verify evolution of the VL structure in low fields.

Note added: Recently, formally similar conclusions about possible VL structures in *d*-wave materials were reported by I. Affleck, M. Franz, and M. Amin [Phys. Rev. B **55**, R705 (1997)]. The authors derive L equations starting with the GL free energy phenomenologically amended with higher-order gradients. For $\mathbf{H}\|\hat{c}$, the single vortex field is given by an equation similar to Eq. (8). For certain choices of the parameters involved, the energy minimization yields the square VL which transforms to *H*-dependent structures in low fields.

The authors thank J. Clem and P. Canfield for informative discussions and interest in this work. The work at Ames was supported by the Office of Basic Energy Sciences, DOE, and in part (V.K.) by the NSF Grant No. DMR9307581. The work of P.M. was supported in part by the International Institute of Theoretical and Applied Physics at ISU, Ames.

[1] U. Yaron, P. L. Gammel, A. P. Ramirez, D. A. Huse, D. J. Bishop, A. I. Goldman, C. Stassis, P. C. Canfield, K. Mortensen, and M. R. Eskildsen, Nature (London) **382**, 236 (1996).

[2] M. R. Eskildsen, P. L. Gammel, B. P. Barber, U. Yaron, A. P. Ramirez, D. A. Huse, D. J. Bishop, C. Bolle, C. M. Lieber, S. Oxx, S. Sridhar, N. H. Andersen, K. Mortensen, and P. C. Canfield, Phys. Rev. Lett **78**, 1968 (1997).

[3] M. Yethiraj, D. McK. Paul, C. V. Tomy, and E. M. Forgan (unpublished).

[4] Y. De Wilde *et al.* (unpublished).

[5] M. Tinkham, *Introduction to Superconductivity* (McGraw-Hill, New York, 1996).

[6] A. A. Abrikosov, *Fundamentals of the Theory of Metals* (North-Holland, New York, 1988).

[7] K. Takanaka, in *Anisotropy Effects in Superconductors*, edited by H. Weber (Plenum, New York, 1977), p. 93; J. Schelten, *ibid.*, p. 113.

[8] L. J. Campbell, M. Doria, and V. G. Kogan, Phys. Rev. B **38**, 2439 (1988).

[9] V. G. Kogan, L. N. Bulaevskii, P. Miranović, and Lj. Dobrosavljević-Grujić, Phys. Rev. B **51**, 15 344 (1995).

[10] D. K. Christen, H. R. Kerchner, S. T. Sekula, and P. Thorel, Phys. Rev. B **21**, 102 (1980).

[11] D. K. Christen, H. R. Kerchner, S. T. Sekula, and Y. K. Chang, Physica B **135**, 369 (1985).

[12] V. G. Kogan, A. Gurevich, J. H. Cho, D. C. Johnston, Ming Xu, J. R. Thompson, and A. Martynovich, Phys. Rev. B **54**, 12 386 (1996).

[13] V. G. Kogan, P. Miranović, Lj. Dobrosavljević-Grujić, W. E. Pickett, and D. K. Christen (unpublished).

[14] V. G. Kogan, Phys. Rev. B **24**, 1572 (1981).

[15] W. Weber (private communication).

[16] L. Mattheiss, Phys. Rev. B **49**, 13 279 (1994).

[17] S. L. Bud'ko and P. C. Canfield (private communication).

[18] H. Takagi, R. J. Cava, H. Eisaki, J. O. Lee, K. Mizuhashi, B. Batlogg, S. Uchida, J. J. Krajewski, and W. F. Peck, Jr., Physica C **228**, 389 (1994).